https://doi.org/10.5194/egusphere-2026-3793
Preprint. Discussion started: 10 July 2026

Beyond Linear Scaling: Dynamical Controls on European Precipitation Extremes

Tugba Ozturk[1,2], Dominic Matte[3], Jens Hesselbjerg Christensen[4]

[1]Department of Physics, Faculty of Engineering and Natural Sciences, Isik University, 34980 Istanbul, Turkey
[2]Department of Engineering Sciences, Faculty of Engineering, Abdullah Gül University, Kayseri, 38080, Turkey
[3]Ouranos, 550 Rue Sherbrooke W., West Tower, 19th Floor, Montréal, QC H3A 1B9, Canada
[4]Physics of Ice, Climate and Earth, Niels Bohr Institute, University of Copenhagen, Copenhagen, Denmark

Correspondence to: Tugba Ozturk (tugbaozturkt@gmail.com)

Abstract. This study investigates the scalability of extreme precipitation indices across the Mediterranean Basin and Europe using 0.11° EURO-CORDEX regional climate model projections. A pattern-scaling framework is applied to assess whether changes in extreme precipitation exhibit a robust relationship with increments in global mean temperature and to determine the time of emergence of scalable patterns during the twenty-first century. Scaling relationships are derived for five extreme precipitation indices using annual mean global temperature change from the driving global climate models.

A clear distinction emerges between ensemble-mean behavior and individual model responses. For most indices, the ensemble mean converges toward the late-century pattern relatively early in the century, suggesting that large-scale thermodynamic control linked to global warming governs the forced signal in precipitation extremes. Individual model realizations, however, display substantially greater spread and often lack a stable scaling relationship until much later in the century.

Projected changes reveal a pronounced north–south contrast across Europe, with increasing precipitation extremes in northern regions and progressively drier conditions across much of the Mediterranean Basin and southern Europe. However, the analysis shows that precipitation extremes do not conform uniformly to a linear scaling with global mean temperature. In contrast to temperature-based metrics, a robust linear relationship for precipitation emerges only gradually and remains weak or absent for the most extreme indices.

Crucially, the breakdown of linear scaling is not merely a limitation of the framework, but a physically informative signal indicating a transition in the controlling mechanisms of precipitation extremes. The forced thermodynamic response becomes clearly distinguishable from internal variability by around mid-century, but for the most extreme events, the deviation from scalable behavior reflects an increasing dominance of regional circulation changes and large-scale dynamical adjustments over thermodynamic constraints alone. In this regime, departures from scaling capture the growing influence of atmospheric dynamics rather than uncertainty.

By the late century, projected changes in several indices remain broadly consistent with large-scale patterns of change, yet the least scalable metrics highlight where dynamical processes override temperature-driven expectations. As a result, some precipitation metrics can be linked to warming more directly than others. This distinction has important implications for

https://doi.org/10.5194/egusphere-2026-3793
Preprint. Discussion started: 10 July 2026

pattern-scaled projections, as the breakdown of scaling provides insight into when and where atmospheric dynamics become the primary control on European precipitation extremes, rather than representing noise around a simple thermodynamic response.

Keywords: Climate change, regional climate modeling, extreme precipitation indices, EURO-CORDEX, Mediterranean Basin.

1 Introduction

The IPCC AR6 infers that anthropogenic global warming is modifying the global hydrological cycle, increasing its variability and thereby amplifying both precipitation extremes and drought occurrence (IPCC, 2021). Climate model projections indicate increasing mean precipitation at high latitudes, contrasted by widespread decreases across the subtropics, including most of the Mediterranean Basin. An exception is found in northern Mediterranean areas, such as the Alpine region, where winter precipitation is anticipated to rise. In contrast, warm-season precipitation is projected to decline across the Mediterranean Basin, with the strongest reductions occurring during summer (Giorgi and Coppola, 2007; Mariotti et al., 2015; Lionello and Scarascia, 2018; André et al., 2024).

Multi-model assessments estimate an average decrease in Mediterranean precipitation of approximately 4% per 1 °C increase in global mean temperature (Lionello and Scarascia, 2018), accompanied by a robust increase in interannual variability, particularly in regions experiencing pronounced drying (Giorgi and Bi, 2005). Across Europe more broadly, projections consistently indicate decreasing summer precipitation in southern regions and increasing precipitation in northern Europe, alongside a widespread intensification of extreme precipitation events with regard to both frequency and magnitude (Christensen and Christensen, 2007; Fischer and Schär, 2010; Rajczak and Schär, 2017; Matte et al., 2019; Di Sante et al., 2021).

While atmospheric warming also intensifies global annual precipitation, significant uncertainties persist at both regional and seasonal levels, especially regarding extreme weather events. Due to the serious environmental and economic impacts of extreme precipitation events, future changes in extreme precipitation and their uncertainties have received considerable attention. The intensity of extreme precipitation is regulated by atmospheric moisture and is anticipated to scale with warming by about 6–7% per 1 °C of warming, regarding the Clausius-Clapeyron relationship under the premise of constant relative humidity. (Allan and Soden, 2008; Allen and Ingram, 2002; Trenberth, 2011). In contrast, alterations in total precipitation are controlled by the Earth's energy balance, and at the global scale, changes in global mean precipitation are relatively slow, with increases estimated at around 1–3% per degree of warming (Douville et al., 2021).

Although models generally show agreement in the direction of future precipitation changes, they differ in magnitude owing to uncertainties in external forcing, model climate sensitivity, and the internal variability of the climate system (Hawkins and Sutton, 2009). To interpret such variations, Santer et al. (1990) introduced the pattern-scaling approach, which assumes a linear link between regional climate change and global mean temperature. The method provides spatial projections of

https://doi.org/10.5194/egusphere-2026-3793
Preprint. Discussion started: 10 July 2026

climate change per degree of warming and serves as a cost-effective alternative to high-resolution regional modeling (Lustenberger et al., 2014; Herger et al., 2015), enabling the estimation of climate impacts for scenarios without requiring direct simulations. Large international projects such as CMIP, PRUDENCE, ENSEMBLES, and CORDEX have advanced its use. Studies show that pattern scaling performs reliably for temperature and, with some uncertainty, for precipitation (e.g. Christensen et al. 2015), and is generally not strongly affected by the choice of emission scenario (Tebaldi and Arblaster, 2014; Christensen et al., 2019; Matte et al., 2019; Ozturk et al., 2023).

Christensen et al. (2019) demonstrated that the pattern-scaling method is a reliable approach for projecting temperature and precipitation changes, showing robustness (i.e., consistency across models) across different projects such as PRUDENCE, ENSEMBLES, and CORDEX and across a range of spatial resolution within CORDEX. Their study also found strong agreement between model outputs and observation-based products, supporting the assumption of a linear relationship between European temperature rise and global warming that could hold until the late century. However, since models need time to reach equilibrium, and given that the reference period may be insufficiently separated in time, the emergence of this linearity may be delayed, and the reliability of signals must always be judged in relation to inter-model variability.

A key question is whether this assumption remains valid for precipitation extremes. Unlike temperature, whose response to external forcing is largely governed by thermodynamic processes and therefore exhibits a relatively smooth relationship with global mean warming, precipitation is additionally influenced by changes in atmospheric circulation, moisture transport, convection, and land–atmosphere feedback. These processes introduce substantial spatial heterogeneity and internal variability, particularly in regions such as the Mediterranean Basin, where thermodynamic and dynamic influences may act in opposing directions. Consequently, precipitation extremes provide a stringent test of the extent to which regional climate responses can be represented as a simple and approximately linear function of global mean temperature change.

The pattern-scaling method has been applied not only to mean changes in climate variables but also to changes in extremes. Lustenberger et al. (2014) examined extreme weather events using the pattern-scaling method, which employed daily temperature outputs from 12 RCMs within the ENSEMBLES project. They tested two future time periods, scaling against 2021–2050 or 2070–2099 relative to 1961–1990, and showed that both performed well across most regions, even for percentile-based indices. Since the study focused on RCMs, regional temperature changes rather than global warming were used as the scaling parameter. The authors highlighted that uncertainties increase when the response period is near the reference period due to shifts in the temperature distribution. Skill was higher for indices based on the upper tail of the distribution.

Another study applied the pattern-scaling method to simulate changes in climate extreme indices, using the NCAR-DOE CESM1-CAM5 (CESM) model (Hurrell et al., 2013) and the Large Ensemble (LENS) simulations (Kay et al., 2015). Although the study mainly focused on error metrics, after testing simulation performance across a wide range of indices, it concluded that the simple pattern-scaling approach is successful for most temperature and precipitation indices (Tebaldi et al., 2020). Ozturk et al. (2023) applied scaling of extreme temperature indices with global mean warming and confirmed a near-linear relationship between regional extremes and global temperature rise. Their results show that in Europe, the coldest

https://doi.org/10.5194/egusphere-2026-3793
Preprint. Discussion started: 10 July 2026

night (TNn) warms more than the hottest day (TXx). The ensemble mean signal emerges as early as 2020, while individual model scaled patterns for TNn and TXx become evident around 2040.

Bador and Alexander (2022) analyzed outputs from 29 CMIP6 models by using PRCPTOT and RX1DAY as measures of total and extreme precipitation respectively. They show that the wettest day of the year is expected to become more intense across land in the extratropical regions of the Northern Hemisphere, as well as during the monsoon over India, in all seasons. Decreases in extreme precipitation intensity were expected in some subtropical regions, including large areas around the Mediterranean Basin and southern Africa; however, these drying signals were not as pronounced in annual total precipitation. To account for differences in warming levels across models, the future relative changes in precipitation indices were normalized by regional mean temperature increase using the same 30-year climatology for historical and future periods. As in Lustenberger et al. (2014), warming levels were calculated regionally rather than globally. The study demonstrated that CMIP6 projections of future changes in both total and extreme precipitation scale with warming. Across all four seasons, the intensification of both mean and extreme precipitation over land across the extratropics of the Northern Hemisphere was emphasized as a thermodynamic response to rising surface temperatures (e.g., Bador et al., 2018; Pfahl et al., 2017).

In a study comparing CMIP3, CMIP5, CMIP6, and HighresMIP with ENSEMBLES and EURO-CORDEX datasets, changes in precipitation were analyzed over different periods (Ritzhaupt and Maraun, 2023). Projected changes were expressed relative to the European mean warming to minimize the impact of climate sensitivity and to facilitate comparisons across forcing scenario generations. All ensembles assessed agreed on large-scale patterns of change in mean and extreme daily precipitation, but significant inconsistencies remained at regional scales. Inconsistencies within and across ensembles were most pronounced in summer. A notable discrepancy was found in the strength of Mediterranean drying, as CMIP5 and EURO-CORDEX consistently produced less severe drying than the remaining ensembles. Another discrepancy was found in Eastern Europe, where all ensembles except EURO-CORDEX projected a summer decrease in precipitation. According to this study, regional climate models tend to shift global climate model outputs toward wetter changes (Ritzhaupt and Maraun, 2023). The increase was anticipated in daily extreme precipitation across much of Europe, but with varying magnitudes across models and ensembles. The reliability of this signal was found to be low in the Mediterranean due to the few wet days. The spread in projections of extreme precipitation, both within and across ensembles, was greater than for mean precipitation, especially in summer.

Ritzhaupt and Maraun (2024) applied the pattern-scaling method to CMIP5 and CMIP6 global climate model ensembles, to separate uncertainties in extreme daily precipitation projections into thermodynamic and dynamic contributions. According to the multi-model projection averages, dynamical factors account for most of total uncertainty, especially over tropical and subtropical regions but uncertainties associated with thermodynamic processes are generally smaller. Relative to CMIP5, CMIP6 projections exhibited lower uncertainties in both thermodynamic and dynamic responses somewhat over mid- and high latitudes, while significant reductions in dynamic uncertainties were found over the tropics and subtropics.

As the studies above demonstrate, pattern scaling has increasingly been applied to extreme climate indices. Nevertheless, important uncertainties remain regarding its applicability to precipitation extremes, which are strongly influenced by

https://doi.org/10.5194/egusphere-2026-3793
Preprint. Discussion started: 10 July 2026

atmospheric dynamics and internal variability. The present study therefore examines the extent to which changes in European precipitation characteristics can be represented as scalable responses to global mean temperature change. To provide a stringent test of the scaling assumption, the analysis focuses on simulations under strong radiative forcing, thereby maximizing the forced signal relative to internal variability.

Specifically, we investigate three related questions: (i) whether changes in selected precipitation indices exhibit robust scaling behaviour with global warming, (ii) whether different classes of precipitation indices show different degrees of scalability, and (iii) when the climate-change signal emerges above internal variability and becomes robustly detectable. To address these questions, we analyze five ETCCDI precipitation indices derived from the EURO-CORDEX ensemble using a pattern-scaling framework based on global mean temperature change.

2 Materials and methods

2.1 Datasets

In this study, outputs from the EURO-CORDEX regional climate model projections (Jacob et al., 2014) are analyzed at a horizontal resolution of 0.11° (~12 km) grid mesh. Daily precipitation from 60 global–regional model pairs is examined under the high-emission scenario RCP8.5 for the period 1981–2100 (Fig. 1). The choice of a high-emission scenario is not intended to represent a most likely future pathway, but rather to maximize the forced climate signal relative to internal variability, thereby enabling a more robust assessment of scaling relationships and their structural stability across models. To evaluate model performance and contextualize simulated changes, results are compared against observations from the ERA5 reanalysis dataset (Hersbach et al., 2023). ERA5 daily total precipitation is used for the period 1951–2025.

https://doi.org/10.5194/egusphere-2026-3793
Preprint. Discussion started: 10 July 2026

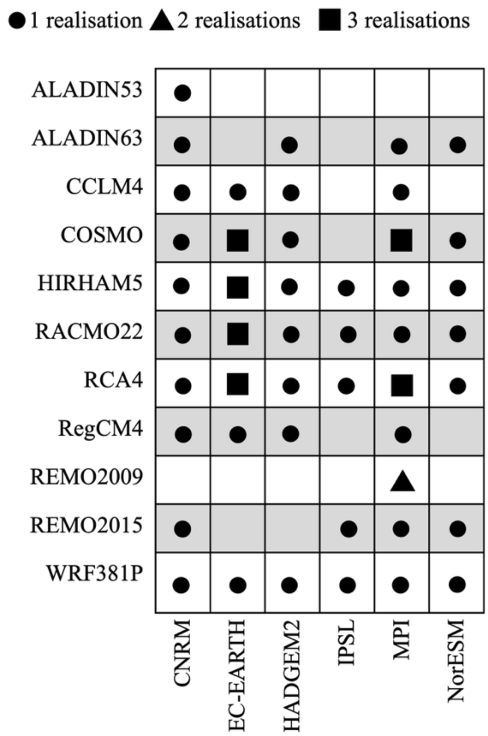

Figure 1: GCM/RCM Matrix.

2.2 Methodology

2.2.1 Extreme precipitation indices

Using the daily total precipitation outputs, five extreme climate indices defined by the ETCCDI (Alexander et al., 2006; Klein Tank et al., 2009; Zhang et al., 2011) were computed. Changes in extreme precipitation indices were calculated relative to 1985–2004. These indices have been widely adopted in the last decade (Sillmann and Roeckner, 2008; Sillmann et al., 2013a, 2013b; Chen and Sun, 2014; Fischer and Knutti, 2014; Islam et al., 2015; Lee et al., 2020; Ntoumos et al., 2020; Shawul and Chakma, 2020; Chervenkov and Slavov, 2021; Ozturk et al., 2021). The indices used in this study are the following: PRCPTOT, the annual total precipitation on wet days; CDD, consecutive dry days, the maximum number of consecutive days with precipitation < 1 mm; R95p, very wet days, annual total precipitation from days when daily precipitation exceeds the 95th percentile of the reference period (1985-2004) in percentage of days, R10mm, heavy precipitation days, the number of days when daily total precipitation > 10 mm, and PRMAX, the annual maximum precipitation.

https://doi.org/10.5194/egusphere-2026-3793
Preprint. Discussion started: 10 July 2026

2.2.2 The scaling approach

This paper investigated how changes in extreme precipitation indices respond to global warming, as obtained by their corresponding driving global climate models, using a pattern-scaling approach. In this method, the scaled signal for each index was computed by dividing its 20-year mean change (relative to the reference period, 1985–2004) by the respective global mean temperature increase projected by the relevant GCM. This pattern-scaling approach assumes a direct, proportional relationship between regional climate responses and global warming. The method first involves calculating the 20-year running-mean changes for each index from regional climate model simulations through the end of the century. These regional changes were then divided by the associated 20-year mean global temperature change derived from the respective GCM in the GCM-RCM pair. For instance, for the RegCM4.0 simulation driven by the HadGEM2-ESM-MR, the scaling parameter was computed from the HadGEM2-ESM-MR global temperature trajectory. This approach enabled an evaluation of how strongly changes in extreme precipitation indices correlate with an increase in global mean temperature.

2.2.3 Signal-to-noise ratio (S/N)

The robustness of regional climate model outputs was assessed by calculating the signal-to-noise ratio (S/N). For each scaled field, the S/N was computed as:

$$S/N = \frac{\langle SP \rangle}{\sigma_{SP}} \quad (1)$$

where $\langle SP \rangle$ represents the mean of the scaled patterns across all model outputs, and σ_{SP} is the inter-model standard deviation of the scaled patterns (Christensen et al., 2019). This method assesses the reliability of the climate change signal. After calculating the changes in 20-year moving averages, each 20-year mean was compared with the end-of-century average (2080–2099). The purpose of this comparison is to determine the year when a potential linear or other relationship between global temperature rise and changes in extreme precipitation indices first emerges.

3 Results

Future changes in five extreme precipitation indices were calculated from daily precipitation values from the EURO-CORDEX simulations at ~12 km grid mesh for the period 1981–2100 under the RCP8.5 scenario. For each index, the changes in the scaled patterns were first computed at the end of the century, then, throughout the century, the correlation between the scaled patterns and the end-of-century signal was evaluated. All changes are represented relative to 1985–2004. In all maps, gray shading indicates areas with S/N<1, showing the level of robustness of the scaled signal.

3.1 Simulations of PRCPTOT

3.1.1 Change in Scaled Patterns of PRCPTOT Index at the End of the Century

https://doi.org/10.5194/egusphere-2026-3793
Preprint. Discussion started: 10 July 2026

The PRCPTOT index, representing the annual total precipitation on wet days, was computed by summing the daily precipitation amounts for each year. Changes for every 20 years were calculated as a percentage relative to the reference period and then scaled to account for global temperature increase. The end-of-the-century scaled signal is shown in the multi-model outputs (Fig. 2). The scaled multi-model signal reveals a dipolar-like precipitation pattern, with pronounced wetting over the interior of northern Scandinavia, the northern Baltic Sea gulfs, and northern Iceland, and weaker increases extending across northern Germany, the Czech Republic, Poland, and northern Ukraine. The increase in precipitation over the northern half of the domain appears robust, given the S/N ratio (no gray shading). The north of the Mediterranean Basin, namely southern Europe, is shown as a transition region where change transforms from increase to no change and eventually to decrease. It is also the region where the signal may be considered less robust, as gray shading indicates a low S/N ratio due to almost no change in precipitation. The robust decreases are anticipated over the southern Mediterranean, most notably over North Africa. Considering the S/N ratio, this reduction is robust and consistent across models. These findings have also been stated in model-based projections of precipitation changes over Europe for both summer and winter (Christensen et al., 2019).

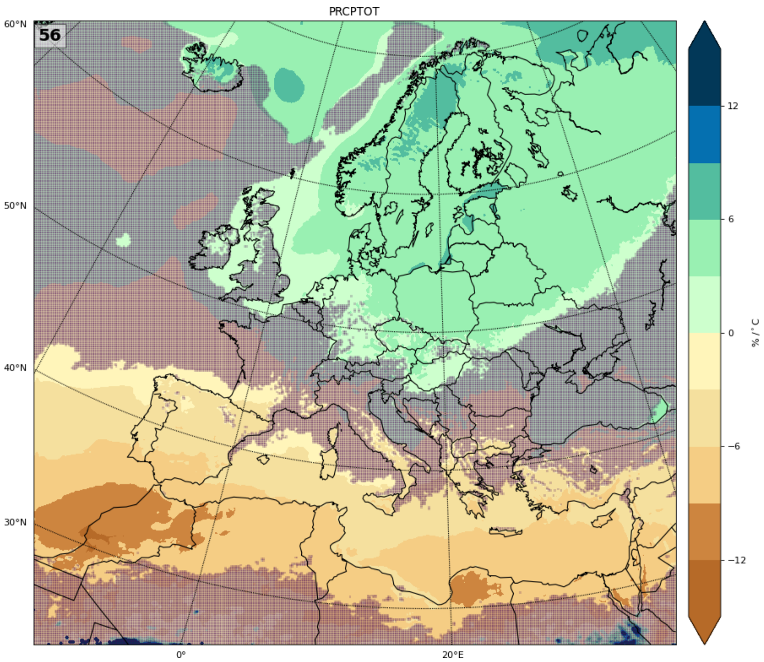

Figure 2: Percentage change in the multi-model mean scaled patterns of the PRCPTOT index for 2080–2099 relative to 1985–2004. The number in the upper-left corner shows the percentage of grid points where S/N > 1.

Seasonal means of the PRCPTOT index were also investigated to see the seasonal pattern of the scaled signal (Fig. 3). A more pronounced increase over the northern portion of the region is anticipated in winter and spring, whereas drier conditions are seen over the Mediterranean regions. Drying conditions are shifted toward the north, including France, northern Italy, the Balkan countries, and even the southern part of the UK. The transition zone is also shifted north and

https://doi.org/10.5194/egusphere-2026-3793
Preprint. Discussion started: 10 July 2026

narrowed in the summer. We note that the apparent increase over the Sahara is related to the very low overall precipitation there, leading to very noisy fluctuations in relative precipitation changes, and should be discarded.

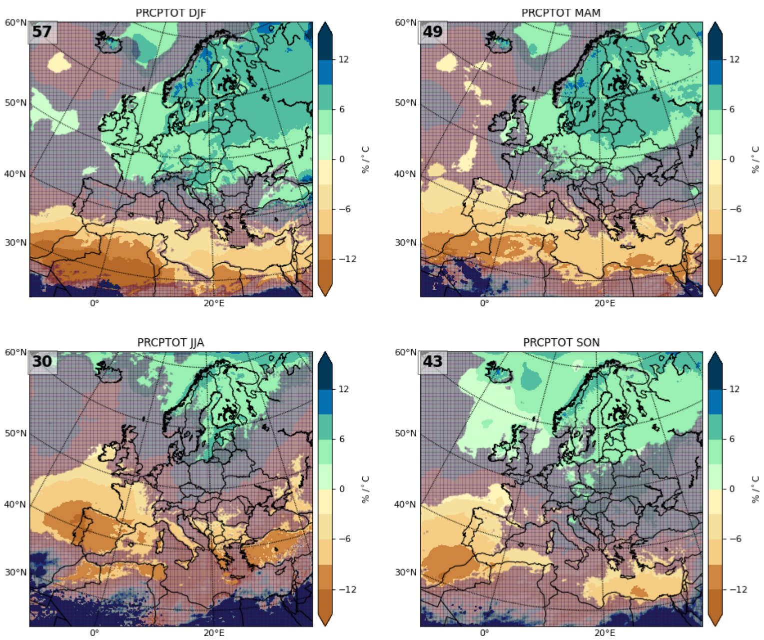

Figure 3: Percentage change in the multi-model mean scaled patterns of the seasonal PRCPTOT index for 2080–2099 relative to 1985–2004. The number in the upper-left corner shows the percentage of grid points where S/N > 1.

3.1.2 Emergence of the End-of-Century Scaled Pattern of the PRCPTOT Index

A video animation has been produced to illustrate the emergence of the scaled signal in the end-of-century changes of the PRCPTOT index (SuppVideo 1). The results show that the late-century change signal is expected to appear as early as around the year 2030. A robustness assessment indicates that, because the decrease in precipitation is not substantial, the point at which the signal rises above the noise (S/N > 1) is expected to occur around 2050 over North Africa and in northern and central Europe. Notably, over the Mediterranean, the signal remains too weak to be considered robust by the S/N metric. The scaled end-of-century signal, characterized by a dipole of wet and dry conditions, begins to emerge even before it is deemed robust according to this metric. To assess the temporal emergence of the end-of-the-century pattern for both the multi-model mean and the individual model pair, spatial correlations relative to the end-of-the-century pattern were calculated across the century (Fig. 4). Similar findings are reflected in the correlation graph of the PRCPTOT index, where both the ensemble mean and individual model pairs demonstrate high correlations around 2040.

https://doi.org/10.5194/egusphere-2026-3793
Preprint. Discussion started: 10 July 2026

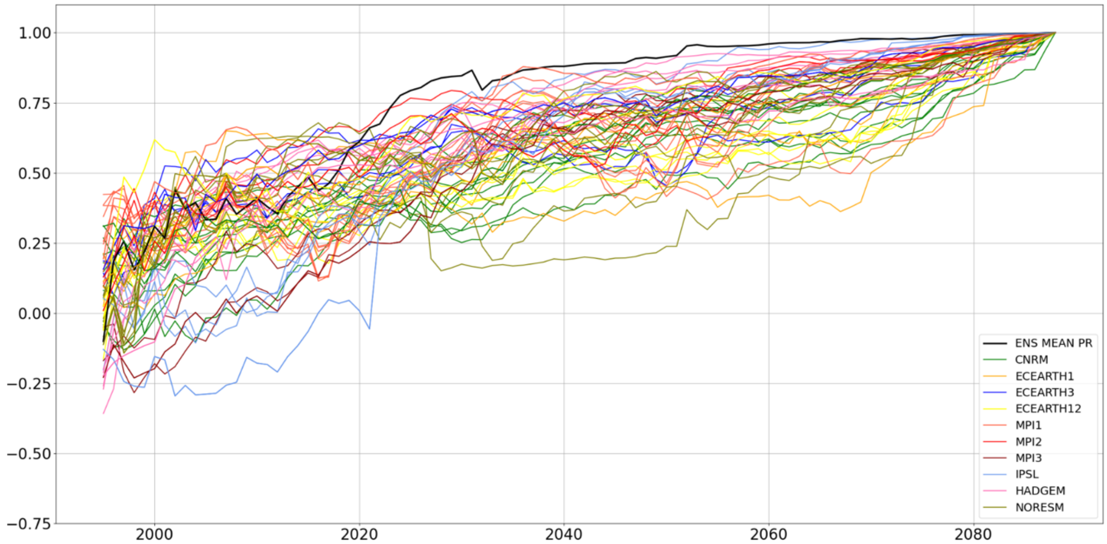

Figure 4: Correlation between the 20-year moving averages of the scaled patterns of individual models and the multi-model mean (black line) with the end-of-century (2080–2099) signal for the PRCPTOT index from 1990 onwards. For simplicity, only the driving data are mentioned in the legend.

3.1.3 Investigation of Observed Changes in the PRCPTOT Index Using the ERA5 Dataset

To assess whether the end-of-century-scale signal has already been observed in past conditions, changes in the total precipitation index PRCPTOT were analyzed using the ERA5 dataset. Figure 5 illustrates the change in the PRCPTOT index for 2006–2025 relative to the 1951–1970 period, expressed both as a percentage (Fig. 5a) and in millimeters (Fig. 5b). The spatial patterns of projected and observed changes show broad agreement for the PRCPTOT index. Notably, the anticipation of wetter conditions in the northern portion of the region and drier conditions in the southern portion has already been realized in observed conditions. Specifically, the UK, Iceland, Scandinavia, and central Europe experienced a marked increase in annual total precipitation (Fig. 5b). In percentage terms, an increase of approximately 20% is observed over the mentioned region (Fig. 5a). Even though this change does not match the magnitude of the scaled end-of-century model pattern, it reflects a similar directional trend (Fig. 5).

Additionally, the observational data indicate that dry conditions have already been experienced in North Africa and the Mediterranean, aligning well with late-century patterns. The multi-model signal also projects wetter conditions over Iceland and the North Atlantic Ocean, consistent with the observed change in the region. Overall, although the late-century pattern is not identical to observed conditions, it can reasonably be interpreted as projecting similar conditions.

https://doi.org/10.5194/egusphere-2026-3793
Preprint. Discussion started: 10 July 2026

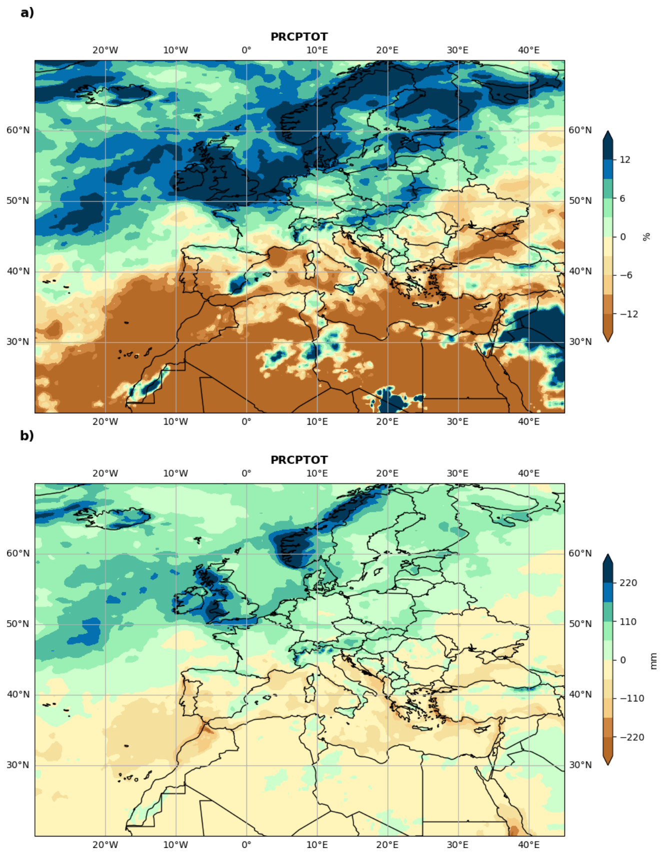

Figure 5: The change in PRCPTOT index in (a) % and (b) mm for 2006–2025 relative to 1951–1970 using the ERA5 dataset.

3.2 Simulations of CDD Index

3.2.1 Scaled Patterns of the CDD Index at the End of the Century

The CDD index provides information on long-term drought and its severity. Results are presented as changes in the maximum number of consecutive dry days in a year per unit increase in global temperature (Fig. 6). In the late century, the scaled pattern shows positive changes or no change in CDD in almost all parts of the region, except for a few days of decrease over Scandinavia and the northernmost part of the domain. Northern Europe is expected to experience no change in CDD, which, together with the increase in PRCPTOT presented in the previous section, indicates that precipitation increases are not distributed across more days, but rather arise from more intense events. However, the southern part of the domain is expected to have longer consecutive dry days. A higher increase is anticipated as one goes further south. Most Mediterranean countries will experience severe droughts, according to the projections. In the Mediterranean Basin, drought events are expected to span 6 to 8 days longer per year per degree of global warming.

https://doi.org/10.5194/egusphere-2026-3793
Preprint. Discussion started: 10 July 2026

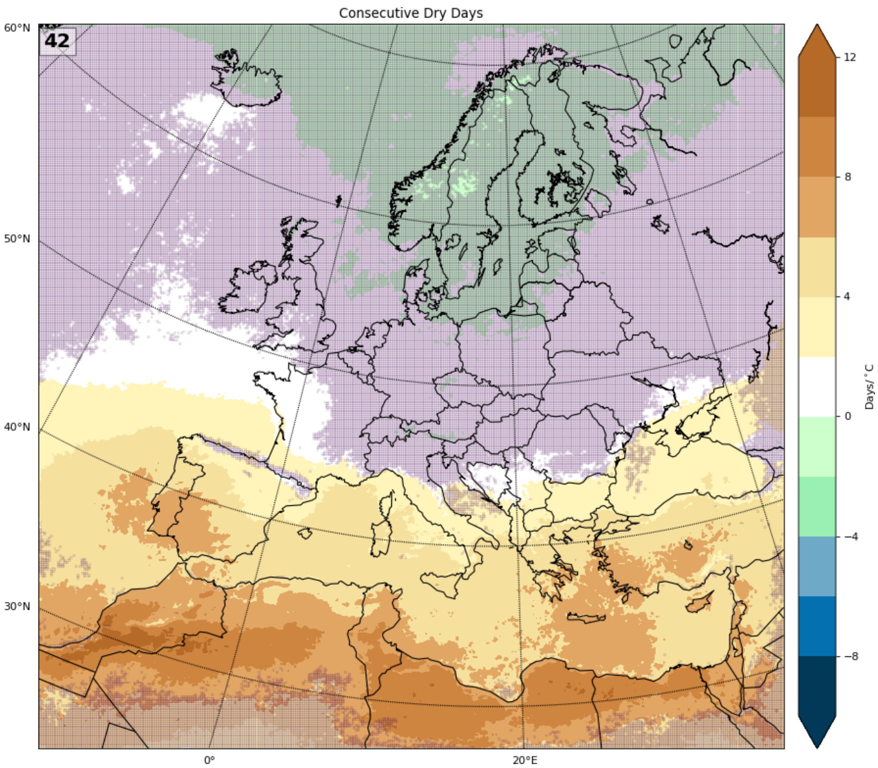

Figure 6: Scaled pattern changes of the CDD index (in days/°C) for 2080–2099 relative to 1985–2004. The number in the upper-left corner shows the percentage of grid points where S/N > 1.

3.2.2 Emergence of the End-of-Century Scaled Pattern of the CDD Index

The emergence of the scaled signal projected by individual model pairs and the ensemble mean of model results for the CDD index by the end of the century was illustrated through a video animation (SuppVideo 2), which displays its temporal evolution. Compared to the PRCPTOT index (SuppVideo 1), the change in the number of CDD emerges much earlier, around 2010, for each degree of global warming. The increase in the CDD over the Mediterranean Basin, North Africa, and Southern Europe is evident in model results from an early stage. Likewise, the projection of no change for the northern part of the region also emerges very early. The spatial correlation between the 20-year running mean of the model average and the end-of-century pattern yields similar results (Fig. 7). The model average (black line) reaches high values around 2010. When examining the correlations of individual model pairs with their end-of-century patterns, a different picture emerges. Although models produce similar results, their correlation values reach high levels only after around 2040 (Fig. 7).

https://doi.org/10.5194/egusphere-2026-3793
Preprint. Discussion started: 10 July 2026

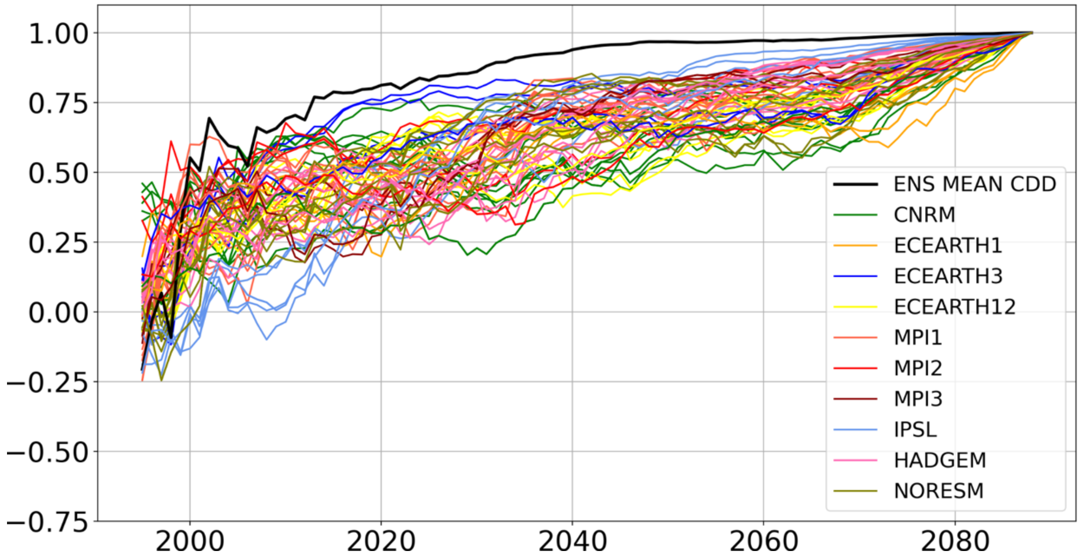

Figure 7: Correlation of 20-year moving averages of scaled patterns from individual models of the CDD index with the model average (black line) and the end-of-century (2080–2099) levels, from 1990 to the end of the period.

3.3 Simulations of R95p Index

280 #### 3.3.1 Scaled Patterns of the R95p Index at the End of the Century

The very wet days index is defined as the percentage of annual precipitation that falls on days exceeding the 95th percentile of the reference period. Model results state that the late-century scaled pattern projects positive changes in the R95p index across most of the region, except for the Sahara (Fig. 8). The near-zero changes in the Sahara result from the region's already arid conditions with little to no precipitation. Although the increase in very wet days is minor over the Mediterranean Basin, it is projected to be larger over Northern Europe. Across most of the domain, very wet days are expected to increase by about 0.5% to 2.0% per degree of global warming by the late century. The projected response closely aligns with that obtained for the PRCPTOT index.

https://doi.org/10.5194/egusphere-2026-3793
Preprint. Discussion started: 10 July 2026

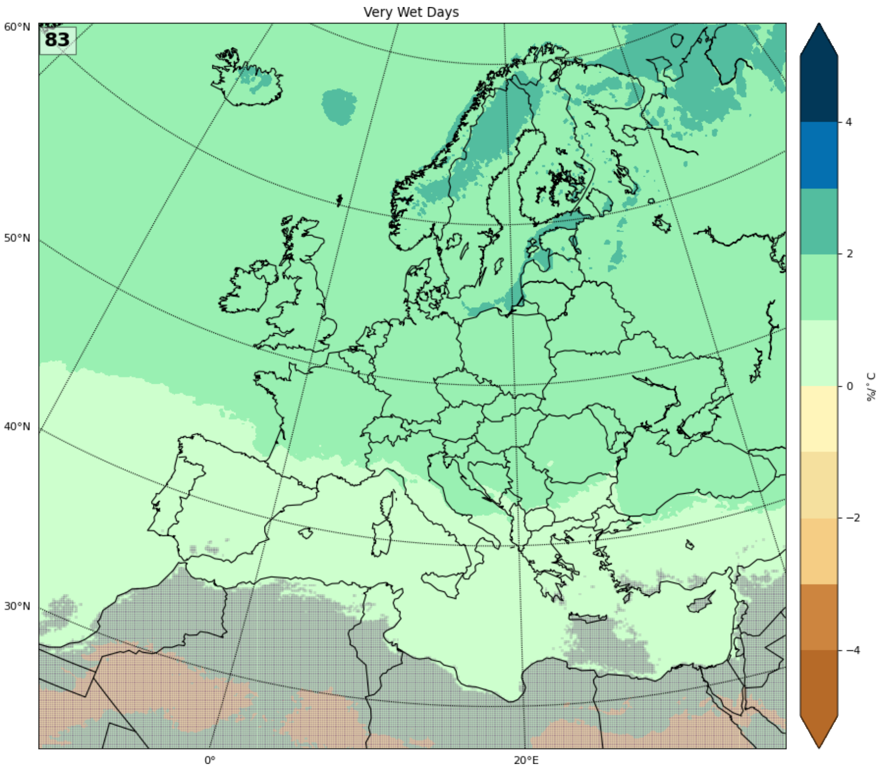

Figure 8: Scaled pattern changes of very wet days (R95p) index (in %/°C) for 2080–2099 relative to 1985–2004. The number in the upper-left corner shows the percentage of grid points where S/N > 1.

3.3.2 Emergence of the End-of-Century Scaled Pattern of the R95p Index

The video animation shows the emergence of the scaled signal for the R95p index, as presented in SuppVideo 3. Throughout the century, positive values indicating increased heavy precipitation have been observed in the region. By the late century, the scaled pattern showing stronger increases in Northern Europe emerges around 2025 in the animation. In the animation, the projected increase in magnitude changes over time. A smooth pattern of change is evident in the signal. This is also clearly reflected in the correlation graph for the late-century scaled-pattern signal (Fig. 9). The average of all models has been correlated with the late-century signal almost from the beginning (around 2005). However, the R95p index increases more slowly than the global temperature change. For individual model pairs, high correlation values are observed for most models around 2020, while by 2040, all models reach these values. Additionally, the correlation graph indicates that regional climate model signals are GCM-driven (same colors, same path).

https://doi.org/10.5194/egusphere-2026-3793
Preprint. Discussion started: 10 July 2026

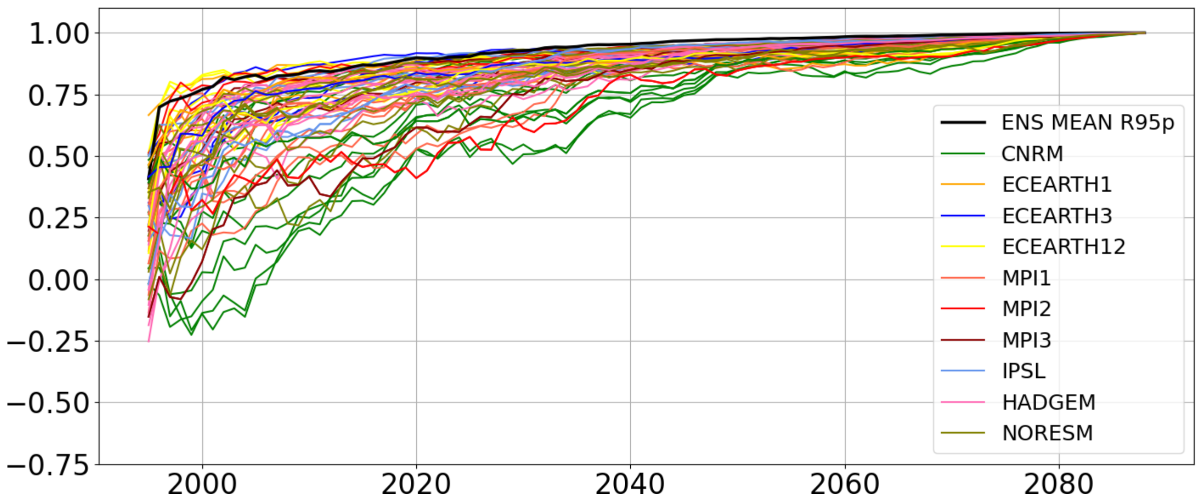

Figure 9: Correlation of 20-year moving averages of scaled patterns from individual models of the R95p index with the model average (black line) and the end-of-century (2080–2099) levels, from 1990 to the end of the period.

305 ## 3.4 Simulations of R10mm Index

3.4.1 Scaled Patterns of the R10mm Index at the End of the Century

In the R10mm index, 10 mm daily precipitation is defined as a heavy precipitation threshold. The scaled changes in this index in the late century, relative to global warming, are shown in Fig. 10. The region again exhibits a clear bipolar pattern consistent with the PRCPTOT index. With each degree of global warming, the number of heavy precipitation days decreases
310 in the Mediterranean Basin and increases in Northern Europe. Particularly, decreases are more pronounced in the Mediterranean coastal areas and the Iberian Peninsula, while increases in heavy precipitation days are clearly observed in Scandinavia (Fig. 10).

https://doi.org/10.5194/egusphere-2026-3793
Preprint. Discussion started: 10 July 2026

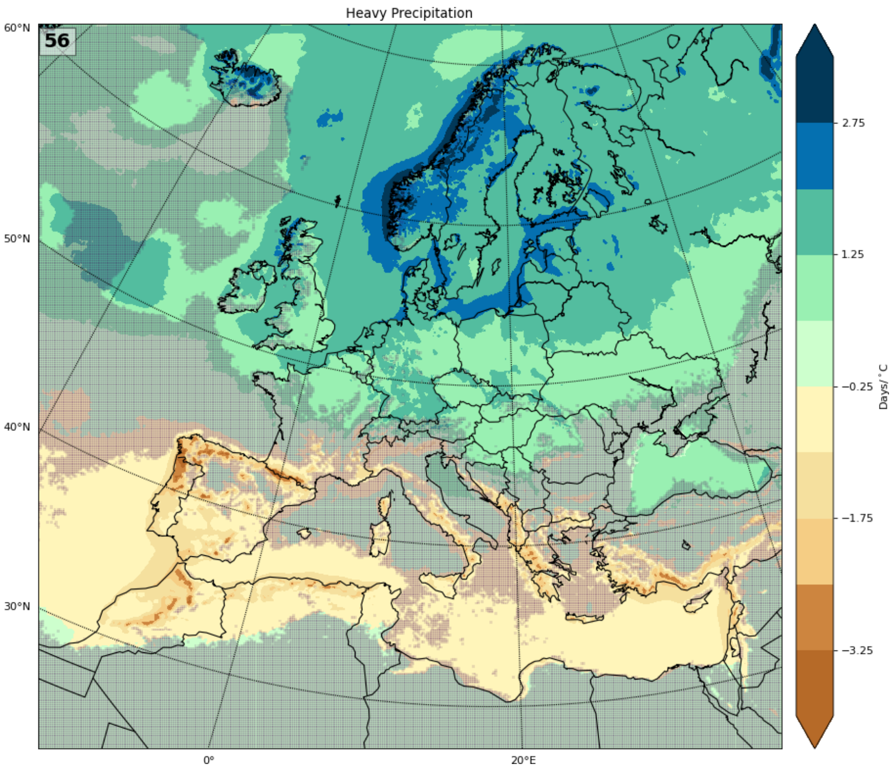

Figure 10. Scaled pattern changes of heavy precipitation days (R10mm) index (in days/°C) for 2080–2099 relative to 1985–2004. The number in the upper-left corner shows the percentage of grid points where S/N > 1.

3.4.2 Emergence of the End-of-Century Scaled Pattern of the R10mm Index

The emergence of the scaled end-of-century pattern of the R10mm index was evaluated using an animation (SuppVideo 4) covering changes throughout the century. The late-century pattern of heavy precipitation days, particularly the increases in the north, appears as early as around 2010. Similarly, decreases observed in the Mediterranean coastal areas and the Iberian Peninsula emerge around 2020. This is also clearly reflected in the correlation graph with the end-of-century signal (Fig. 11). The model average (black line) shows high values starting around 2010. According to individual model results, almost all models reach high correlations by 2040. Initially, models run with the CNRM dataset do not correlate, but they converge with other model results around 2045.

https://doi.org/10.5194/egusphere-2026-3793
Preprint. Discussion started: 10 July 2026

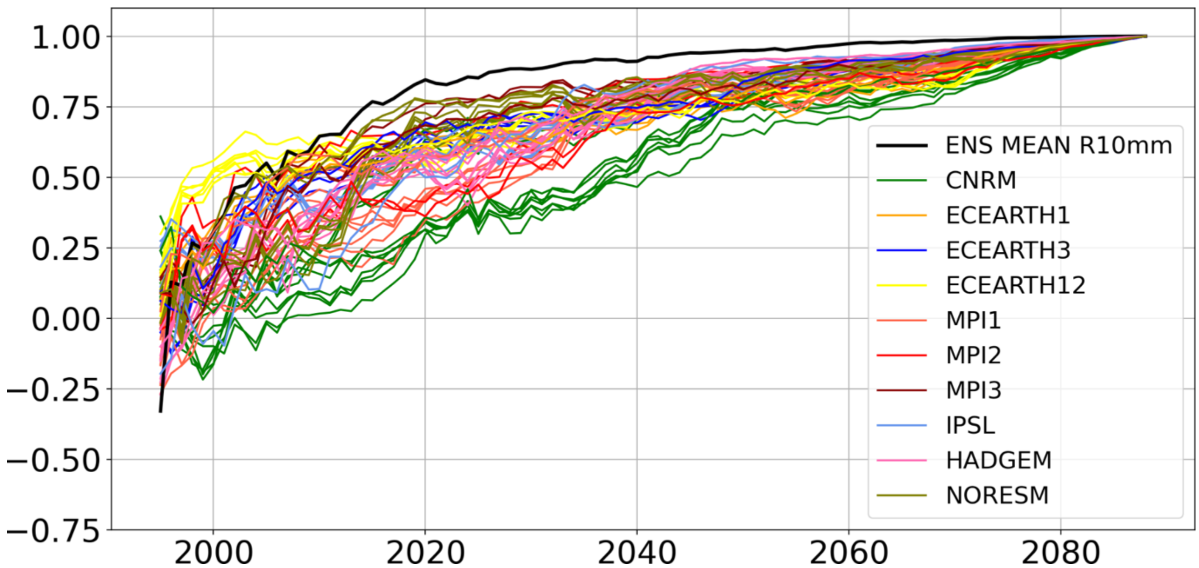

325 **Figure 11: Correlation of 20-year moving averages of scaled patterns from individual models of the R10mm index with the model average (black line) and the end-of-century (2080–2099) levels, from 1990 to the end of the period.**

3.5 Simulations of the Annual Maximum Precipitation (PRMAX)

3.5.1 Scaled Patterns of the Annual Maximum Precipitation (PRMAX) at the End of the Century

A change in PRMAX projections for the late century is shown in Fig. 12. Across most of the region, an increase in PRMAX is projected. The spatial pattern of change is consistent with results from other heavy precipitation indices (R95p, R10mm), with a stronger increase in the northern part, as observed in this index. The projected change is strengthening across the north. Although dry conditions are expected over the Mediterranean region, projections still indicate an increase in extreme precipitation, reflecting a tendency for such events to intensify even in dry areas. The expected change in Northern Africa is from a minor change to no change, consistent with the region's already low precipitation regime.

https://doi.org/10.5194/egusphere-2026-3793
Preprint. Discussion started: 10 July 2026

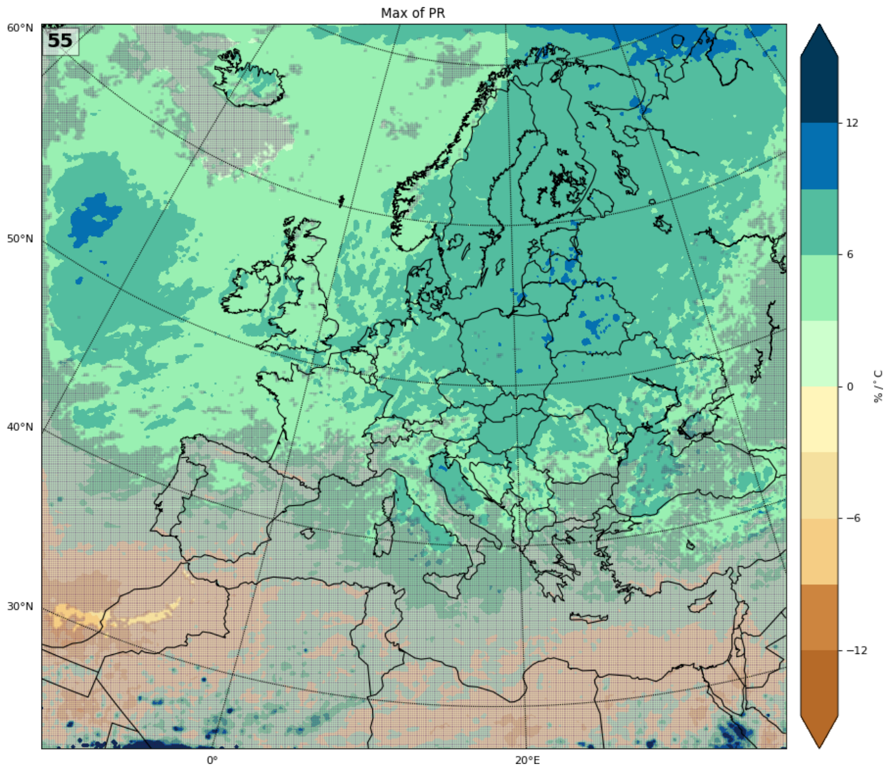

Figure 12: Scaled pattern changes of the annual maximum precipitation (in %/°C) for 2080–2099 relative to 1985–2004. The number in the upper-left corner shows the percentage of grid points where S/N > 1.

3.5.2 Emergence of the End-of-Century Scaled Pattern of the Annual Maximum Precipitation (PRMAX)

The temporal evolution of the scaled end-of-century PRMAX pattern was investigated using an animation (SuppVideo 5). Even though the ensemble mean of the model results shows emergence around 2040, consistent with the correlation graph for the ensemble mean (Fig. 13), the individual regional climate model results show no correlation until the moving window begins to overlap with the late-century window. Substantial inter-model variability persists, reflecting the high internal variability for this index. The ensemble mean of the model projections tells a different story than the individual model pairs. Low correlation values indicate that the assumption of a scalable response does not hold for the most extreme precipitation.

https://doi.org/10.5194/egusphere-2026-3793
Preprint. Discussion started: 10 July 2026

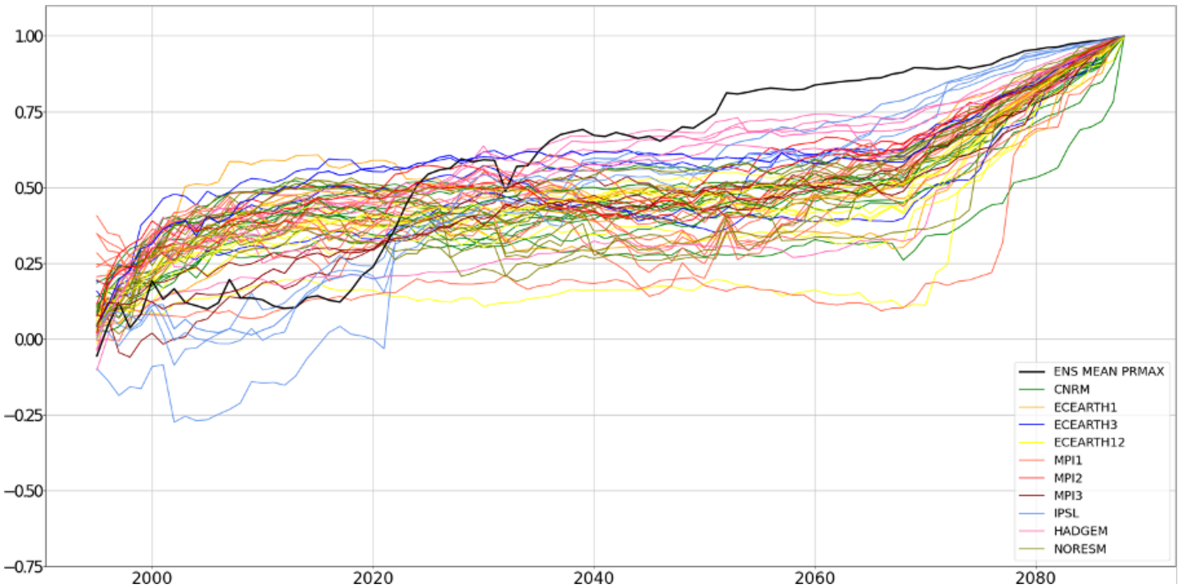

Figure 13: Correlation of 20-year moving averages of scaled patterns from individual models of PRMAX with the model average (black line) and the end-of-century (2080–2099) levels, from 1990 to the end of the period.

4 Discussion and Conclusion

Five extreme precipitation indices derived from daily total precipitation outputs of regional climate models were analyzed for the period 1981–2100 under RCP8.5. Future changes in these indices relative to the 1985–2004 period were examined using 20-year moving averages across the century. Model agreement was assessed using the signal-to-noise ratio, defined as the ensemble-mean change relative to inter-model standard deviation. Signals were considered robust where $S/N > 1$. Changes in each index analyzed were expressed as scaled patterns (change per global mean warming [°C]). This supports pattern scaling as a first-order approximation for mean precipitation and some moderate extremes. However, the analysis also reveals systematic and spatially coherent deviations from this behaviour, indicating that precipitation responses cannot be understood by thermodynamic constraints alone. The relationship between extreme precipitation indices and global temperature was diagnosed using 20-year moving averages and their correlation with end-of-century patterns. Scaled responses emerge at different times across indices, with precipitation extremes generally lagging temperature-driven signals by several decades.

The ensemble mean shows a strong correlation with late-century scaled patterns, indicating that large-scale forced signals are robust across models. However, when looking at individual models, some pairs show a positive correlation by the end of the century, while others do not. Thus, relying solely on the ensemble mean warrants careful evaluation. Moreover, when applying the pattern-scaling method, early minor deviations in the pattern toward the late century can have a significant influence, as the global temperature change used for scaling remains small at first (<1°C) and fluctuates year to year. Early

https://doi.org/10.5194/egusphere-2026-3793
Preprint. Discussion started: 10 July 2026

differences in models, i.e., noise signals, appear in animations and correlation graphs. Even if the signal is initially absent, it later demonstrates its relationship with the late-century values.

Since the ensemble mean of scaled patterns represents ratios that emerged early in the century, model results were compared with observations from the ERA5 dataset, selected for its high resolution and established suitability for climate analysis. Daily total precipitation was calculated for the period 1951–2025, and changes were computed from 2006–2025 relative to 1951–1970. The last 20-year changes reflect strong recent warming and provide insights into end-of-century conditions. Observed changes, while not identical to projections, show broad qualitative agreement with end-of-century scaled patterns, particularly in terms of increased drying in the Mediterranean Basin, and enhanced precipitation in northern Europe.

The five precipitation indices can be grouped into wet and dry categories, with CDD representing the sole dry-condition metric. Substantial increases in CDD are projected in North Africa, the Mediterranean Basin, and Southern Europe, emerging early in the century. For total precipitation (PRCPTOT), results also indicate decreasing precipitation totals in southern regions, consistent with a drying tendency. R95p, R10mm, and PRMAX represent wet conditions with increases in extreme precipitation primarily in Northern Europe, and the strongest amplification is found in annual maximum precipitation (PRMAX). Scaled precipitation patterns emerge later than temperature-based indices (Ozturk et al., 2023), around the 2040 median year. Although the relationship with global mean temperature increase is weaker than for temperature indices, it becomes evident by mid-century in the ensemble mean. Ensemble-mean signals emerge earlier than those of individual model pairs, reflecting the damping of internal variability through averaging. PRCPTOT shows a relatively strong correlation with late-century patterns, whereas PRMAX exhibits weak and inconsistent scaling across individual model pairs. Taking the ensemble mean of the signal, especially for this index, suppresses the different individual signals, particularly for PRMAX. When calculating the change in the number of days or the percentage of days, rather than the change in intensity, individual model correlations with late-century patterns increase substantially after ~2040. The R95p index is an exception, showing relatively strong agreement with late-century spatial patterns but weaker consistency in scaling with global mean temperature. Time-evolution diagnostics indicate a visually smooth emergence of the signal; the change signal is considered smooth and correlates well; however, the increase in the percentage of wet days greater than the 95th percentile of the reference period is not at the same rate as the global mean temperature increase. This indicates that pattern scaling does not suit this index well.

Pattern scaling seems less successful for extreme precipitation indices over Europe, particularly in the Mediterranean Basin. Weak correlation, especially for the PRMAX index, indicates a significant limitation of the pattern-scaling approach for extreme precipitation. For the PRMAX index case, correlation begins to increase as the time window approaches the late century. The agreement with the end-of-century pattern is likely attributable to internal variability or noise rather than to a clear signal of forced climate change. This behavior differs from that of temperature-based indices, which show an earlier emergence of the late-century signal. Extreme precipitation indices often show a belated, less pronounced response to global temperature increases. The PRMAX index stresses the limited pertinence of linear scaling to variables whose governing processes are nonlinear and strongly influenced by regional dynamics.

https://doi.org/10.5194/egusphere-2026-3793
Preprint. Discussion started: 10 July 2026

From a physical perspective, these results reflect the interplay between thermodynamic constraints, primarily governed by the Clausius–Clapeyron relationship, and dynamically mediated changes in atmospheric circulation. While thermodynamic scaling provides a useful baseline expectation for moisture availability, regional precipitation responses are strongly modulated by changes in vertical motion, moisture convergence, and large-scale circulation patterns. The deviations identified here can therefore be interpreted as dynamically induced departures from thermodynamic scaling.

Extreme precipitation over Europe, particularly in the Mediterranean Basin, is governed by both thermodynamic and dynamic factors, whose relative effects vary in space and time. Unlike temperature extremes, which are solely controlled by thermodynamics and consequently scale linearly with global temperature increases, extreme precipitation is modulated by complex interactions among atmospheric moisture availability, circulation dynamics, and land-atmosphere feedback. Even though global warming increases atmospheric moisture availability, depending on Clausius-Clapeyron scaling (6–7% $°C^{-1}$), and enhances heavy precipitation, the occurrence and intensity of extreme precipitation events are heavily controlled by vertical motion, storm-track variability, and convection, and orographic effects, which display internal variability and nonlinear responses to climate forcing (O'Gorman and Schneider, 2009; Trenberth, 2011; IPCC, 2021).

Precipitation extremes are strongly affected by the interactions between soil moisture and the atmosphere over the Mediterranean region. Future drying conditions are expected to lower evapotranspiration rates and alter the partitioning of surface energy, increasing sensible heat flux relative to latent heat flux. This shift can lead to a warmer and more stable boundary layer, which may prevent convective development even in a warmer atmosphere capable of holding more moisture (Seneviratne et al., 2010; Giorgi & Lionello, 2008; IPCC, 2021). As a result, changes in surface conditions may offset expectations of stronger precipitation extremes under warming, thereby weakening a simple linear relationship between global temperature increases and regional precipitation intensity. In addition, changes in large-scale atmospheric circulation also play an important role. Projected poleward shifts of midlatitude storm tracks, expansion of the subtropical dry zones, and more persistent blocking patterns can influence where and how intense precipitation occurs, often independently of the magnitude of global warming (Ulbrich et al., 2009; Shepherd, 2014; IPCC, 2021).

An implicit assumption underlying pattern scaling is the linearity of regional responses in relation to global mean temperature. The present results suggest that this assumption holds to first order across large spatial scales but becomes increasingly strained in regions where circulation changes intensify with warming. This highlights that strong forcing scenarios not only improve signal detection but also provide a useful stress test of the linearity assumption itself.

A large part of the spread in precipitation extremes can be traced to dynamical factors and to how models handle convection. Compared with temperature, precipitation is much more sensitive to these processes, making the results less consistent across models. This is especially noticeable in the earlier decades, when the warming signal is still relatively weak and easily masked by natural variability. For this reason, the relationship between scaled precipitation extremes and global temperature does not appear particularly stable at first glance. The increase in correlation observed toward the end of the century, therefore, likely reflects the gradual emergence of the thermodynamic signal above internal variability rather than a stable linear scaling relationship throughout the entire period. Overall, these results suggest that pattern scaling is more reliable for

https://doi.org/10.5194/egusphere-2026-3793
Preprint. Discussion started: 10 July 2026

temperature-related variables, whereas its application to precipitation extremes is more challenging. In regions like the Mediterranean, where atmospheric circulation, surface conditions, and moisture availability are tightly linked, scaled precipitation indices should therefore be interpreted carefully and supported by a physical understanding of the underlying processes.

Here, we evaluated the applicability of pattern scaling to extreme precipitation using a large ensemble of global–regional climate model simulations under RCP8.5. Large-scale precipitation responses show a first-order linear relationship with global mean temperature, supporting the use of pattern scaling for mean changes and some moderate extremes. However, this relationship weakens substantially for intensity-based extremes, particularly maximum daily precipitation, and in regions such as the Mediterranean Basin.

Deviations from linear scaling are spatially coherent and reflect systematic differences in modeled atmospheric circulation responses rather than random variability. These results demonstrate that precipitation extremes are governed by a combined thermodynamic–dynamic framework, where circulation changes play a critical role in shaping regional outcomes. Overall, pattern scaling is a useful but limited approximation: robust for large-scale signals but insufficient to represent the nonlinear behavior of extreme precipitation in dynamically sensitive regions.

Code and data availability

The EURO-CORDEX regional climate simulations analyzed in this study are available on the Earth System Grid Federation website (https://esgf-data.dkrz.de/projects/cordexdkrz/). The code used in this study can be obtained from the corresponding author upon reasonable request. The video animations supporting this study are publicly available from the Zenodo repository (DOI:10.5281/zenodo.20931644).

Author contributions

JHC conceived the idea and contributed to the review and editing. TO led the study, performed the analysis, and led the writing. DM contributed to the analysis, reviewing, and editing. All authors contributed to the article and approved the submitted version.

Competing interests

The authors declare no conflicts of interest.

Acknowledgements

The analysis presented in this paper was performed entirely at TUBITAK ULAKBIM High Performance and Grid Computing Center (TRUBA resources).

Financial Support

This study was funded by the Scientific and Technological Research Council of Turkey (TUBITAK) ARDEB 3501 Grant No 121Y587.

References

Alexander, L. V., Zhang, X., Peterson, T. C., Caesar, J., Gleason, B., Tank, A. M. G. K., Haylock, M., Collins, D., Trewin, B., Rahimzadeh, F., et al.: Global observed changes in daily climate extremes of temperature and precipitation, J. Geophys. Res., 111, D05109, https://doi.org/10.1029/2005JD006290, 2006.

Allan, R. P. and Soden, B. J.: Atmospheric warming and the amplification of precipitation extremes, Science, 321, 1481–1484, https://doi.org/10.1126/science.1160787, 2008.

Allen, M. R. and Ingram, W. J.: Constraints on future changes in climate and the hydrologic cycle, Nature, 419, 224–232, https://doi.org/10.1038/nature01092, 2002.

André, J., d'Andrea, F., Drobinski, P., and Muller, C.: Regimes of precipitation change over Europe and the Mediterranean, J. Geophys. Res. Atmos., 129(15), e2023JD040413, https://doi.org/10.1029/2023JD040413, 2024.

Bador, M., Donat, M. G., Geoffroy, O., and Alexander, L. V.: Assessing the robustness of future extreme precipitation intensification in the CMIP5 ensemble, J. Climate, 31(16), 6505–6525, https://doi.org/10.1175/JCLI-D-17-0683.1, 2018.

Bador, M. and Alexander, L. V.: Future seasonal changes in extreme precipitation scale with changes in the mean, Earth's Future, 10(12), e2022EF002979, https://doi.org/10.1029/2022EF002979, 2022.

Chen, H., Sun, J., and Chen, X.: Projection and uncertainty analysis of global precipitation-related extremes using CMIP5 models, Int. J. Climatol., 34, 2730–2748, https://doi.org/10.1002/joc.3871, 2014.

Chervenkov, H. and Slavov, K.: ETCCDI climate indices for assessment of the recent climate over southeast Europe, in: Advances in High Performance Computing: Results of the International Conference on High Performance Computing, Borovets, Bulgaria, 2019, edited by: Dimov, I., Fidanova, S., Springer International Publishing, 398–412, https://doi.org/10.1007/978-3-030-55347-0_34, 2021.

Christensen, J. H. and Christensen, O.: A summary of the PRUDENCE model projections of changes in European climate by the end of this century, Clim. Change, 81, 7–30, https://doi.org/10.1007/s10584-006-9210-7, 2007.

Christensen, J. H., Larsen, M. A. D., Christensen, O. B., Drews, M., and Stendel, M.: Robustness of European climate projections from dynamical downscaling, Clim. Dynam., 53, 4857–4869, https://doi.org/10.1007/s00382-019-04831-z, 2019.

https://doi.org/10.5194/egusphere-2026-3793
Preprint. Discussion started: 10 July 2026

Christensen, O. B., Yang, S., Boberg, F., Fox Maule, C., Olesen, M., Drews, M., Sørup, H. J. D., and Christensen, J. H.: Scalability of Regional Climate Change in Europe for High-End Scenarios, Clim. Res., 64, 25–38, https://doi.org/10.3354/cr01286, 2015.

Di Sante, F., Coppola, E., and Giorgi, F.: Projections of river floods in Europe using EURO-CORDEX, CMIP5 and CMIP6 simulations, Int. J. Climatol., 41(5), 3203–3221, https://doi.org/10.1002/joc.7014, 2021.

Douville, H., Raghavan, K., Renwick, J., Allan, R. P., Arias, P. A., Barlow, M., et al.: Water cycle changes, in: Climate Change 2021: The Physical Science Basis. Contribution of Working Group I to the Sixth Assessment Report of the Intergovernmental Panel on Climate Change, edited by: Masson-Delmotte, V., P. Zhai, A. Pirani, S.L. Connors, C. Péan, S. Berger, N. Caud, Y. Chen, L. Goldfarb, M.I. Gomis, M. Huang, K. Leitzell, E. Lonnoy, J.B.R. Matthews, T.K. Maycock, T. Waterfield, O. Yelekçi, R. Yu, and B. Zhou, Cambridge University Press, Cambridge, United Kingdom and New York, NY, USA, pp. 1055–1210, https://doi.org/10.1017/9781009157896.010, 2021.

Fischer, E. M. and Schaer, C.: Consistent geographical patterns of changes in high-impact European heatwaves, Nat. Geosci., 3, 398–403, https://doi.org/10.1038/ngeo866, 2010.

Fischer, E. M. and Knutti, R.: Detection of spatially aggregated changes in temperature and precipitation extremes, Geophys. Res. Lett., 41, 547–554, https://doi.org/10.1002/2013GL058499, 2014.

Giorgi, F. and Bi, X.: Updated regional precipitation and temperature changes for the 21st century from ensembles of recent AOGCM simulations, Geophys. Res. Lett., 32, L21715, https://doi.org/10.1029/2005GL024288, 2005.

Giorgi, F. and Coppola, E.: European climate-change oscillation (ECO), Geophys. Res. Lett., 34, L21703, https://doi.org/10.1029/2007GL031223, 2007.

Giorgi, F. and Lionello, P.: Climate change projections for the Mediterranean region, Glob. Planet. Change, 63, 90–104, https://doi.org/10.1016/j.gloplacha.2007.09.005, 2008.

Hawkins, E. and Sutton, R.: The potential to narrow uncertainty in regional climate predictions, Bull. Am. Meteorol. Soc., 90, 1095–1108, https://doi.org/10.1175/2009BAMS2607.1, 2009.

Herger, N., Sanderson, B. M., and Knutti, R.: Improved pattern scaling approaches for the use in climate impact studies, Geophys. Res. Lett., 42, 3486–3494, https://doi.org/10.1002/2015GL063569, 2015.

Hersbach, H., Comyn-Platt, E., Bell, B., Berrisford, P., Biavati, G., Horányi, A., Muñoz Sabater, J., Nicolas, J., Peubey, C., Radu, R., Rozum, I., Schepers, D., Simmons, A., Soci, C., Dee, D., Thépaut, J-N., Cagnazo, C., and Cucchi, M.: ERA5 post-processed daily-statistics on pressure levels from 1940 to present. Copernicus Climate Change Service (C3S) Climate Data Store (CDS), https://doi.org/10.24381/cds.4991cf48, (Accessed on 18-12-2025), 2023.

Hurrell, J. W., Holland, M. M., Gent, P. R., Ghan, S., Kay, J. E., Kushner, P. J., et al.: The community earth system model: a framework for collaborative research, Bull. Am. Meteorol. Soc., 94(9), 1339–1360, https://doi.org/10.1175/BAMS-D-12-00121.1, 2013.

IPCC: Climate Change 2021: The Physical Science Basis. Contribution of Working Group I to the Sixth Assessment Report of the Intergovernmental Panel on Climate Change, edited by: Masson-Delmotte, V., Zhai, P., Pirani, A., Connors, S. L., Péan, C., Berger, S., Caud, N., Chen, Y., Goldfarb, L., Gomis, M. I., Huang, M., Leitzell, K., Lonnoy, E., Matthews, J. B. R., Maycock, T. K., Waterfield, T., Yelekçi, O., Yu, R., and Zhou, B., Cambridge University Press, Cambridge, United Kingdom and New York, NY, USA, 2391 pp., https://doi.org/10.1017/9781009157896, 2021.

Islam, M. N., Almazroui, M., Dambul, R., Jones, P. D., and Alamoudi, A. O.: Long-term changes in seasonal temperature extremes over Saudi Arabia during 1981–2010, Int. J. Climatol., 35, 1579-1592, https://doi.org/10.1002/joc.4078, 2015.

Jacob, D., Petersen, J., Eggert, B., Alias, A., Christensen, O. B., et al.: EURO-CORDEX: new high-resolution climate change projections for European impact research, Reg. Environ. Change, 14, 563–578, https://doi.org/10.1007/s10113-013-0499-2, 2014.

Kay, J. E., Deser, C., Phillips, A., Mai, A., Hannay, C., Strand, G., and Vertenstein, M.: The community earth system model (CESM) large ensemble project: A community resource for studying climate change in the presence of internal climate variability, Bull. Am. Meteorol. Soc., 96, 1333–1349, https://doi.org/10.1175/BAMS-D-13-00255.1, 2015.

Klein Tank, A. M. G., Zwiers, F. W., and Zhang, X.: Guidelines on analysis of extremes in a changing climate in support of informed decisions for adaptation, in: Climate Data and Monitoring WCDMP-No. 72, WMO-TD No. 1500, World Meteorological Organization, Geneva, Switzerland, 56, 2009.

Lee, Y., Paek, J., Park, J. S., and Boo, K. O.: Changes in temperature and rainfall extremes across East Asia in the CMIP5 ensemble, Theor. Appl. Climatol., 141, 143–155, https://doi.org/10.1007/s00704-020-03180-w, 2020.

Lionello, P. and Scarascia, L.: The relation between climate change in the Mediterranean region and global warming, Reg. Environ. Change, 18, 1481–1493, https://doi.org/10.1007/s10113-018-1290-1, 2018.

Lustenberger, A., Knutti, R., and Fischer, E. M.: The potential of pattern scaling for projecting temperature-related extreme indices, Int. J. Climatol., 34, 18–26, https://doi.org/10.1002/joc.3659, 2014.

Mariotti, A., Pan, Y., Zeng, N., and Alessandri, A.: Long-term climate change in the Mediterranean region in the midst of decadal variability, Clim. Dynam., 44, 1437–1456, https://doi.org/10.1007/s00382-015-2487-3, 2015.

Matte, D., Larsen, M. A. D., Christensen, O. B., and Christensen, J. H.: Robustness and scalability of regional climate projections over Europe, Front. Environ. Sci., 6, 163, https://doi.org/10.3389/fenvs.2018.00163, 2019.

Ntoumos, A., Hadjinicolaou, P., Zittis, G., and Lelieveld, J.: Updated Assessment of Temperature Extremes over the Middle East–North Africa (MENA) Region from Observational and CMIP5 Data, Atmosphere, 11, 813, https://doi.org/10.3390/atmos11080813, 2020.

O'Gorman, P. A. and Schneider, T.: The physical basis for increases in precipitation extremes in simulations of 21st-century climate change, Proc. Natl. Acad. Sci. U.S.A., 106(35), 14773–14777, https://doi.org/10.1073/pnas.0907610106, 2009.

Ozturk, T., Saygili-Araci, F. S., and Kurnaz, M. L.: Projected Changes in Extreme Temperature and Precipitation Indices Over CORDEX-MENA Domain, Atmosphere, 12(5), 622, https://doi.org/10.3390/atmos12050622, 2021.

Ozturk, T., Canbaz, E., Bilgin, B., Matte, D., Kurnaz, M. L., and Christensen, J. H.: The emergence of projected scaled patterns of extreme temperatures over Europe, Front. Earth Sci., 11, 1178461, https://doi.org/10.3389/feart.2023.1178461, 2023.

https://doi.org/10.5194/egusphere-2026-3793
Preprint. Discussion started: 10 July 2026

Pfahl, S., O'Gorman, P. A., and Fischer, E. M.: Understanding the regional pattern of projected future changes in extreme precipitation, Nat. Clim. Change, 7, 423–427, https://doi.org/10.1038/nclimate3287, 2017.

Rajczak, J. and Schär, C.: Projections of future precipitation extremes over Europe: a multimodel assessment of climate simulations, J. Geophys. Res. Atmos., 122(20), 10773-10800, https://doi.org/10.1002/2017JD027176, 2017.

Ritzhaupt, N. and Maraun, D.: Consistency of seasonal mean and extreme precipitation projections over Europe across a range of climate model ensembles, J. Geophys. Res. Atmos., 128, e2022JD037845, https://doi.org/10.1029/2022JD037845, 2023.

Ritzhaupt, N. and Maraun, D.: State-of-the-art climate models reduce dominant dynamical uncertainty in projections of extreme precipitation, Environ. Res. Clim., 3(2), 021001, https://doi.org/10.1088/2752-5295/ad2eb2, 2024.

Santer, B. D., Wigley, T. M. L., Schlesinger, M. E., and Mitchell, J. F. B.: Developing Climate Scenarios From Equilibrium GCM Results, Report Max Planck Institut für Meteorologie, Max-Planck-Institut für Meteorologie, 1990.

Seneviratne, S. I., Corti, T., Davin, E. L., Hirschi, M., Jaeger, E. B., Lehner, I., Orlowsky, B., and Teuling, A. J.: Investigating soil moisture–climate interactions in a changing climate, Earth-Sci. Rev., 99, 125–161, https://doi.org/10.1016/j.earscirev.2010.02.004, 2010.

Shawul, A. and Chakma, S.: Trend of extreme precipitation indices and analysis of long-term climate variability in the Upper Awash basin, Ethiopia, Theor. Appl. Climatol., 140, 635–652, https://doi.org/10.1007/s00704-020-03112-8, 2020.

Shepherd, T. G.: Atmospheric circulation as a source of uncertainty in climate change projections, Nat. Geosci., 7, 703–708, https://doi.org/10.1038/ngeo2253, 2014.

Sillmann, J. and Roeckner, E.: Indices for extreme events in projections of anthropogenic climate change, Clim. Change, 86, 83–104, https://doi.org/10.1007/s10584-007-9308-6, 2008.

Sillmann, J., Kharin, V. V., Zhang, X., Zwiers, F. W., and Bronaugh, D.: Climate extremes indices in the CMIP5 multimodel ensemble: Part 1. Model evaluation in the present climate, J. Geophys. Res. Atmos., 118, 1716–1733, https://doi.org/10.1002/jgrd.50203, 2013a.

Sillmann, J., Kharin, V. V., Zwiers, F. W., Zhang, X., and Bronaugh, D.: Climate extremes indices in the CMIP5 multi-model ensemble. Part 2: Future projections, J. Geophys. Res., 118, 2473–2493, https://doi.org/10.1002/jgrd.50188, 2013b.

Tebaldi, C. and Arblaster, J. M.: Pattern scaling: its strengths and limitations, and an update on the latest model simulations, Clim. Change, 122, 459–471, https://doi.org/10.1007/s10584-013-1032-9, 2014.

Tebaldi, C., Armbruster, A., Engler, H. P., and Link, R.: Emulating climate extreme indices, Environ. Res. Lett., 15(7), 074006, https://doi.org/10.1088/1748-9326/ab8332, 2020.

Trenberth, K. E.: Changes in precipitation with climate change, Clim. Res., 47, 123–138, https://doi.org/10.3354/cr00953, 2011.

Ulbrich, U., Leckebusch, G. C., and Pinto, J. G.: Extra-tropical cyclones in the present and future climate: a review, Theor. Appl. Climatol., 96, 117–131, https://doi.org/10.1007/s00704-008-0083-8, 2009.

https://doi.org/10.5194/egusphere-2026-3793
Preprint. Discussion started: 10 July 2026

Zhang, X., Alexander, L., Hegerl, G. C., Jones, P., Tank, A. K., Peterson, T. C., Trewin, B., and Zwiers, F. W.: Indices for monitoring changes in extremes based on daily temperature and precipitation data, WIREs Clim. Change, 2, 851–870, https://doi.org/10.1002/wcc.147, 2011.